

# Kinetic Investigation of the Ligand Dependence of Rabbit Skeletal Muscle Myosin Subfragment 1 Cys-697 and Cys-707 Reactivities<sup>†</sup>

Katherine Polosukhina<sup>‡</sup> and Stefan Highsmith\*

Department of Biochemistry, School of Dentistry, University of the Pacific, San Francisco, California 94115

Received June 9, 1997; Revised Manuscript Received July 24, 1997<sup>®</sup>

**ABSTRACT:** Rate constants for the reactions of Cys-697 and Cys-707 of skeletal muscle myosin subfragment 1 (S1) with *N,N'*-*p*-phenylenedimaleimide (pPDM) and its monofunctional analog phenylmaleimide (PM) were measured for S1 and S1 bound to nucleotides and/or actin. The [pPDM] and [PM] dependencies indicate that prereaction noncovalent complexes of S1 and the alkylating agents form. The rates of the pseudo-first-order reactions of the complexes depend on the nucleotide bound. For pPDM, only the rate constant  $k_a$  (for Cys-707 modification) can be measured. The relative  $k_a$  magnitudes are  $S1 \cdot MgATP\gamma S > S1 \cdot MgADP > S1 \cdot MgPP_i > S1 \cdot MgATP > actin \cdot S1 \cdot MgADP > S1 > actin \cdot S1$  (for which  $k_a \sim 0 \text{ s}^{-1}$ ). For PM, only  $k_a$  can be measured for  $S1 \cdot MgATP\gamma S$  and  $S1 \cdot MgPP_i$ . However, for S1,  $S1 \cdot MgADP$ , and  $S1 \cdot MgATP$ ,  $k_i$  (for the reaction of Cys-697) can also be measured, and it is also nucleotide sensitive. The data are consistent with a mechanism in which pPDM or PM binds S1 near Cys-707 to form a noncovalent complex that reacts at a rate determined by the relative orientation of the cysteine sulfhydryl and the bound reagent. The simplest mechanism for the cross-linking step that reconciles these data with earlier cross-linker length data and with S1–nucleotide atomic structures is one which has pPDM–S1 complexes exist part of the time in conformations having the helical Cys-697/Cys-707–pPDM region converted to a loop structure which cross-links. The fact that rigor actin·S1 is the slowest and the  $S1 \cdot MgATP$  analog  $S1 \cdot MgATP\gamma S$  is the fastest to be cross-linked is discussed in terms of possible energetic roles for helix to loop transitions of the Cys-697/Cys-707 region during the ATP hydrolysis cycle.

The motor domain of rabbit skeletal muscle myosin includes eight cysteines in its heavy chain sequence (1). Chicken skeletal muscle myosin has nine (2). Two of them, Cys-697 and Cys-707, are especially reactive in nucleophilic substitution reactions, with Cys-707 being the more reactive (3). Covalent modification of either Cysteine modifies the MgATPase, CaATPase, and KATPase activities; when both are modified, activity is lost (4). Reporter molecules attached to either cysteine indicate structural displacements occur when nucleotides bind at the ATP site (5–7), suggesting that, although the cysteines are not essential for myosin activity and do not occur in some myosins, their structure is a moving part of the transduction mechanism (8). Bifunctional reagents will cross-link the two cysteines, and the rate is accelerated by bound nucleotide (9). The cysteines are cross-linked by reagents of various lengths, all of which trap the nucleotide in the active site (10).

The cross-linking reaction is of particular interest. The increase in the apparent reaction rate caused by the presence of nucleotide has been interpreted to indicate that, for myosin subfragment 1 (S1),<sup>1</sup> Cys-697 and Cys-707 are farther apart than the length of the cross-linking reagent, but for  $S1 \cdot N$ , a conformational change has brought them closer together (11,

12). The atomic structure of chicken skeletal S1 revealed that the two cysteines are located in  $\alpha$ -helical segments, and the distance between them is indeed longer than the lengths of the cross-linking reagents (13). It was anticipated that the structures of S1–nucleotide complexes would have the helix changed to a structure that has the cysteines close enough together to be cross-linked. However, at least for the truncated catalytic domain of *Dictyostelium* myosin bound to ADP·BeF<sub>x</sub>, ADP·AlF<sub>4</sub>, and PP<sub>i</sub>, the structural counterpart of the Cys-697/Cys-707 region in skeletal muscle myosin remains  $\alpha$ -helical (14–16). There may be no discrepancy, as the cross-linking data are for S1 in solution and the atomic structures are for crystals of nucleotides bound to truncated S1 heavy chains for which no cross-linking experiments have been done. Nonetheless, these results suggest that the cross-linking reaction needs to be investigated further to be understood.

Reported here are measurements of the rate constants for the reactions of Cys-707 and Cys-697 with the bifunctional reagent *p*-phenylenedimaleimide (pPDM), and with its monofunctional structural analog phenylmaleimide (PM), for rabbit skeletal myosin S1 itself and S1 bound to various ligands. The data are interpreted in terms of cross-linking mechanisms that reconcile cross-linking results with other S1 structural data.

## MATERIALS AND METHODS

**Proteins and Chemicals.** Myosin was isolated from New Zealand rabbit dorsal muscle (17). Myosin subfragment 1 was prepared from myosin using papain (18) and purified by size exclusion chromatography (Sephacryl S-400) followed by anion exchange chromatography (19, 20). F-Actin

<sup>†</sup> Supported by NIH Grant AR 42895.

<sup>‡</sup> On leave from the Laboratory of Biophysics, Kol'tsov Institute of Developmental Biology, Russian Academy of Sciences, Moscow, Russia.

<sup>®</sup> Abstract published in *Advance ACS Abstracts*, September 15, 1997.

<sup>1</sup> Abbreviations: ATP $\gamma$ S, adenosine 5'- $\gamma$ -thiotriphosphate;  $k_a$ , rate constant for activation of S1 MgATPase activity;  $k_i$ , rate constant for inactivation of S1 MgATPase activity;  $K_A$ , association constant;  $K_D$ , dissociation constant; PM, phenylmaleimide; pPDM, *N,N'*-*p*-phenylenedimaleimide; PP<sub>i</sub>, pyrophosphate; S1, myosin subfragment 1.

was prepared from rabbit dorsal muscle (21). Experiments were done using mixtures of S1 with its regulatory light chain plus either essential light chain 1 or essential light chain 2 bound. S1 MgATPase activity at 25 °C was typically 0.04–0.05 s<sup>-1</sup>. pPDM and PM were from Aldrich. Other chemicals were the best available commercial grade and were used without further purification.

**MgATPase Measurements.** Steady state S1 MgATPase activities for soluble S1 were determined using a coupled assay system (22).

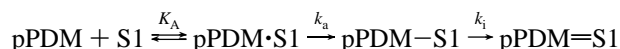
**Chemical Modification of S1.** The cross-linking of the S1 heavy chain reactive thiols Cys-707 and Cys-697 with the bifunctional reagent pPDM was carried out as described by Wells and Yount (10) with some modification. The pH was decreased to 6.8, using the buffer MOPS, to slow the reaction. The extent of cross-linking was monitored by measuring the residual MgATPase activity of aliquots that were quenched with 1 mM  $\beta$ -mercaptoethanol and then diluted 10-fold into the coupled assay solution. The same conditions were used for PM, which also selectively modifies Cys-707 and Cys-697 (37). Control experiments showed that activity changes occurred only when the cross-linking reagent was present.

**Kinetic Analyses.** The MgATPase activity ( $V$ ) of S1, in the presence of pPDM, is given by the equation

$$V = V_o[S1] + V_a[pPDM \cdot S1] + V_i[pPDM=S1] \quad (1)$$

where  $V_o$ ,  $V_a$ , and  $V_i$  are the normal, activated, and inhibited activities of S1, pPDM–S1 (which has only Cys-707 alkylated), and pPDM=S1 (which is cross-linked), respectively. If pPDM and S1 bind to form a noncovalent prereaction complex, pPDM·S1, the reaction scheme is

Scheme 1



for which the rate equations are

$$d[S1]/dt = -k_a[pPDM \cdot S1] \quad (2)$$

$$d[pPDM-S1]/dt = k_a[pPDM \cdot S1] - k_i[pPDM-S1] \quad (3)$$

$$d[pPDM=S1]/dt = k_i[pPDM-S1] \quad (4)$$

If  $[pPDM] \gg 1/K_A$ , and is high enough not to change significantly during the reaction,  $[pPDM \cdot S1] \approx [S1]$ , and the integrated forms of eqs 2–4 are

$$[S1] = [S1]_o \exp(-k_a t) \quad (5)$$

$$[pPDM-S1] = [S1]_o \{ [k_a/(k_i - k_a)] [\exp(-k_a t) - \exp(-k_i t)] \} \quad (6)$$

$$[pPDM=S1] = [S1]_o \{ [1 + 1/(k_a - k_i)] [k_i \exp(-k_a t) - k_a \exp(-k_i t)] \} \quad (7)$$

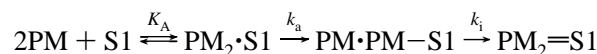
where  $[S1]_o$  is the initial  $[S1]$ .

For the reaction of PM with S1, the observed MgATPase activity,  $V$ , is given by

$$V = V_o[S1] + V_a[PM-S1] + V_i[PM_2=S1] \quad (8)$$

where  $V_o$ ,  $V_a$ , and  $V_i$  are again the normal, activated, and inhibited activities, in this case, of S1, PM–S1 (which has only Cys-707 alkylated), and PM<sub>2</sub>=S1 (which has both Cys-707 and Cys-697 alkylated), respectively. If PM and S1 bind to form a noncovalent prereaction complex, PM<sub>2</sub>·S1, the reaction scheme is

Scheme 2



for which the rate equations are

$$d[PM_2 \cdot S1]/dt = -k_a[PM_2 \cdot S1] \quad (9)$$

$$d[PM \cdot PM-S1]/dt = k_a[PM_2 \cdot S1] - k_i[PM \cdot PM-S1] \quad (10)$$

$$d[PM_2=S1]/dt = k_i[PM \cdot PM-S1] \quad (11)$$

If  $[PM]$  is high enough to saturate S1, then  $[PM_2 \cdot S1] \approx [S1]$  and  $[PM \cdot PM-S1] \approx [PM-S1]$ , and the integrated equations are

$$[S1] = [S1]_o \exp(-k_i t) \quad (12)$$

$$[PM-S1] = [S1]_o \{ [k_a/(k_i - k_a)] [\exp(-k_a t) - \exp(-k_i t)] \} \quad (13)$$

$$[PM_2=S1] = [S1]_o \{ 1 + [k_a/(k_i - k_a)] \exp(-k_i t) - [k_i/(k_i - k_a)] \exp(-k_a t) \} \quad (14)$$

The assumption that S1 binds both reacting PM molecules before the first PM reacts with Cys-707 is arbitrary. However, when  $[PM]$  is large, the alternative scheme in which S1 binds only one PM followed by PM–S1 binding the second PM in a second prereaction equilibrium gives the same integrated rate equations (eqs 12–14), as long as the equilibria are established rapidly.

## RESULTS

**Reaction of pPDM and S1.** The formation of the noncovalent prereaction complex pPDM·S1 is not obligatory, but it does occur. The observed rate of S1 modification increases as  $[pPDM]$  increases up to 30  $\mu$ M, and is constant within experimental uncertainty above 50  $\mu$ M, indicating  $K_D \leq 20 \mu$ M.  $K_D$  was less than 20  $\mu$ M for all the complexes (data not shown).  $K_D$  is not well-defined because the stoichiometry of the complex is not known, but the existence of a complex is consistent with pPDM binding in the probe binding cleft near Cys-707 (24). All the pPDM measurements below were made using 100  $\mu$ M pPDM. Measurements of the rates of modification were also made at increasing nucleotide concentrations to ensure that the active site is saturated (data not shown). These control experiments indicate that it is appropriate to analyze the pPDM data using eqs 1 and 5–7, above.

S1 MgATPase activity at 25 °C was measured at increasing times for aliquots taken from solutions containing 10  $\mu$ M S1 at 2 °C in 50 mM MOPS (pH 6.8), 25 mM Mg(OAc)<sub>2</sub>, 100 mM KOAc, and 100  $\mu$ M pPDM, which were quenched with 1 mM  $\beta$ -mercaptoethanol. Data were collected for S1 and the S1–nucleotide complexes S1·MgADP,

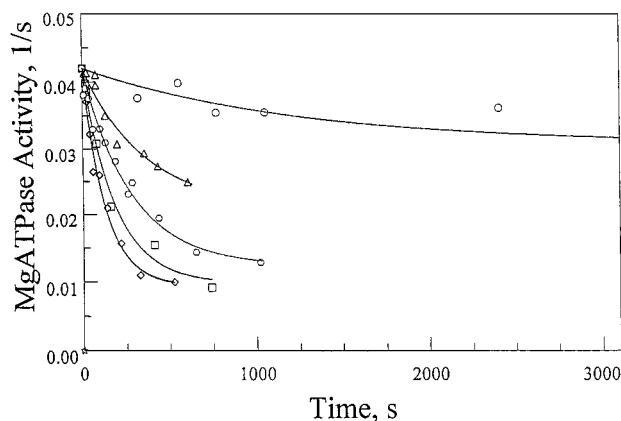


FIGURE 1: pPDM inactivation of S1 and S1–nucleotide complexes. The reaction was started by adding 100  $\mu$ M pPDM to 10  $\mu$ M S1 at 2 °C in 50 mM MOPS, 25 mM Mg(OAc)<sub>2</sub>, 100 mM KOAc, and nucleotide at the concentrations indicated. Aliquots were removed and quenched at the time indicated and assayed for MgATPase activity at 25 °C: no ligand (circles), 10 mM ATP (triangles), 0.10 mM PP<sub>i</sub> (hexagons), 0.10 mM ADP (squares), and 0.10 mM ATP $\gamma$ S (diamonds). The rate constant  $k_a$  was determined (Table 1) as described in the text.

Table 1: pPDM Modification of S1, S1–Nucleotide Complexes, and S1–Actin Complexes

ligand (mM)	$k_a$ ( $\times 10^{-4}$ s <sup>-1</sup> )
none	$7.6 \pm 2.2$
ADP (0.10)	$55 \pm 8$
ATP (10)	$27 \pm 5.4$
ADP·P <sub>i</sub> <sup>a</sup>	$6 \pm 3$
ATP $\gamma$ S (0.10)	$80 \pm 10$
PP <sub>i</sub> (0.10)	$36 \pm 4.1$
ADP and actin (1 and 0.050)	$22 \pm 7.9$
actin (0.050)	$\sim 0$

<sup>a</sup> Estimated from ATP, ADP, and ATP $\gamma$ S data as described in the text. Conditions are given in Figures 1 and 2. Apparent  $K_D$  values are  $<20$   $\mu$ M. See the text for the kinetic scheme used to determine constants.

S1·MgATP, S1·MgATP $\gamma$ S, and S1·MgPP<sub>i</sub> (Figure 1). The MgATPase activity of S1 with only Cys-707 modified is about twice the activity of unmodified S1 (35). Activation of MgATPase activity by pPDM was not detected, in agreement with the results from other laboratories (4). The absence of a detectable activation phase indicates that  $k_i$  is larger than  $k_a$ , in Scheme 1 above. As a result,  $k_i$  cannot be determined for pPDM by this method. In the absence of nucleotide,  $k_a$  is  $7.6 \times 10^{-4}$  s<sup>-1</sup> (Table 1). Although slow, the rate is not negligible, and the data suggest that, whatever the structural change is that enables the two cysteines to come close enough together to react, it occurs in the absence of nucleotide albeit less often than when nucleotide is bound. S1·MgATP has the slowest rate constant of the S1–nucleotide complexes ( $2.7 \times 10^{-3}$  s<sup>-1</sup>), consistent with reports of apparent rates (4, 25). For steady state conditions, S1·MgATP is not the primary species present. At 5 °C, the distribution of S1·MgATP, S1·MgADP·P<sub>i</sub>, and S1·MgADP is approximately 1, 12, and 7 (26), and at 2 °C (the temperature of the pPDM reaction here), it is probably similar. Using this distribution, and assuming the rates in Table 1 for ADP and ATP $\gamma$ S can be used to estimate the S1·MgADP and S1·MgATP contributions, a rate constant  $k_a$  of  $\sim 6 \times 10^{-4}$  s<sup>-1</sup> was calculated for S1·MgADP·P<sub>i</sub>. This is only an estimate and ignores the existence of two S1–MgADP species (27), but it indicates that the value for S1–

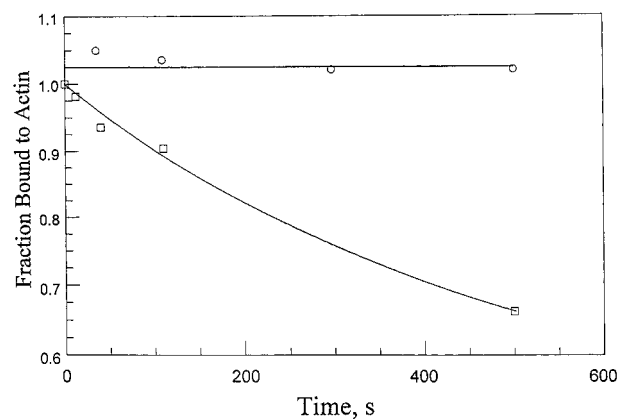


FIGURE 2: pPDM cross-linking of S1 and S1·MgADP bound to actin. The cross-linking of actin-bound S1 and S1·ADP by pPDM was monitored by the loss of actin binding. pPDM (100  $\mu$ M) was added to 5  $\mu$ M S1 plus 50  $\mu$ M actin (circles) or 50  $\mu$ M actin plus 1 mM ADP (squares), in solutions as indicated in Figure 1, except that KOAc was reduced to 5 mM. Aliquots were removed at the time indicated and centrifuged to remove actin and any bound non-cross-linked S1. The [pPDM=S1] in the supernate was assayed by measuring its tryptophan fluorescence intensity. Values of  $k_a$  (Table 1) were determined from the time dependence of the decrease of actin-bound S1.

MgADP·P<sub>i</sub> is considerably smaller than the measured value and comparable to the rate constant determined for S1 (Table 1).

The rate constants increase progressively for S1 bound to PP<sub>i</sub>, ADP, and ATP $\gamma$ S (Figure 1 and Table 1). The fastest rate constant, for S1·MgATP $\gamma$ S, is  $8 \times 10^{-3}$  s<sup>-1</sup>. A problem sometimes encountered using ATP $\gamma$ S is contamination by ADP produced by ATP $\gamma$ S hydrolysis. This is more serious when investigating S1 bound to actin, because the affinities for ADP and ATP $\gamma$ S become comparable (28). If [ADP] were substantial in the present case, it would make the true  $k_a$  for S1·MgATP $\gamma$ S larger than the observed value. The S1 MgATPase activity is 0.011 s<sup>-1</sup>, measured at 2 °C in the buffer used for the pPDM reaction. S1 MgATPase activity is about 69% of S1 MgATPase activity (28), so during the 200 s used to collect data to determine  $k_a$  for ATP $\gamma$ S (Table 1), an estimate of the maximum amount of ADP produced is about 15  $\mu$ M. This assumes there is no loss of activity due to cysteine modification. The actual amount of ADP produced is less, and its effect on  $k_a$  in the presence of the much higher [ATP $\gamma$ S] is negligible.

**pPDM Reaction with S1 and S1·MgADP Bound to Actin.** The cross-linking of Cys-707 to Cys-697 at 2 °C when S1 or S1·MgADP was bound to actin was started by adding 100  $\mu$ M pPDM to 5  $\mu$ M S1, 50  $\mu$ M actin, and 0 or 1 mM ADP. The buffer was the same as that used for the experiments done without actin, except the [KOAc] was reduced to 5 mM. Aliquots were removed and quenched with 1 mM  $\beta$ -mercaptoethanol, and then centrifuged to remove the actin and any pPDM–S1 or S1 bound to it (23). The S1 converted to pPDM=S1 does not bind to actin, and its concentration was determined by measuring the tryptophan fluorescence intensity of the supernatant. Rate constants were determined from the time dependence of pPDM=S1 production (Figure 2).

Binding to actin reduced  $k_a$  for both S1 and S1·MgADP. For S1·MgADP, the  $k_a$  is reduced from  $5.5 \times 10^{-3}$  to  $2.2 \times 10^{-3}$  s<sup>-1</sup>, and for S1, it is reduced from  $7.6 \times 10^{-4}$  to 0 s<sup>-1</sup>, within experimental uncertainty (Table 1). The corrections

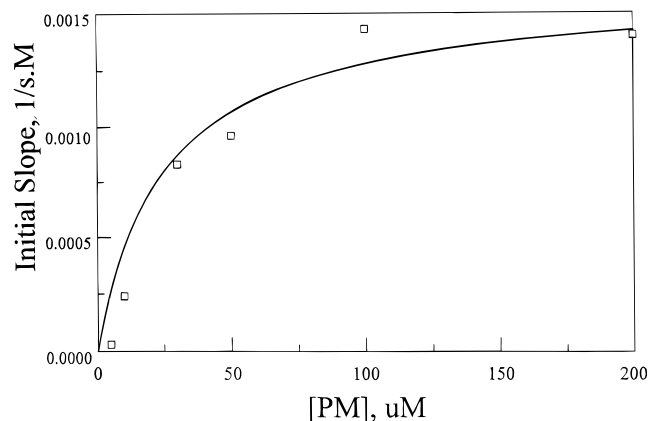


FIGURE 3: [PM] dependence of the activation phase of S1·MgADP modification. The slope of the early portion of PM modification of S1·MgADP is shown for a [PM] in the 5–250  $\mu$ M range. An apparent dissociation constant was estimated from the [PM] that gave 50% of the maximum slope. Conditions were as given in Figure 1.

Table 2: PM Modification of S1 and S1–Nucleotide Complexes<sup>a</sup>

ligand (mM)	$K_D$ ( $\mu$ M)	$k_a$ ( $\times 10^{-4}$ s <sup>-1</sup> )	$V_a$ (s <sup>-1</sup> )	$k_i$ ( $\times 10^{-4}$ s <sup>-1</sup> )
none	58	$22 \pm 6$	$0.079 \pm 0.006$	$1.7 \pm 0.64$
ADP (0.10)	19	$2600 \pm 930$	$0.073 \pm 0.004$	$470 \pm 120$
ATP (10)	5	$310 \pm 150$	$0.060 \pm 0.004$	$56 \pm 2$
ATP $\gamma$ S (0.10)	39	$590 \pm 90$		
PP <sub>i</sub> (0.10)	20	$14 \pm 0.4$		

<sup>a</sup> Conditions are given in Figures 3 and 5. See the text for the kinetic scheme used to determine constants.

for the cross-linking of free S1 or S1·MgADP that is in equilibrium with the actin complex are very small for these conditions (<2% for S1·MgADP and <0.2% for S1) and were not made. Actin reduces, but does not eliminate, modification of Cys-707 of S1 when the modifying reagent is present at concentrations much lower than that used here (29). This result combined with the pPDM data (Table 1) suggests that the conformation that allows cross-linking of Cys-707 to Cys-697 occurs for actin·S1·MgADP but not for actin·S1.

**Reaction of PM and S1.** The monofunctional analog of pPDM, PM, was used in an attempt to resolve the reactivities of the two cysteines and to obtain information about  $k_i$ . Control experiments, analogous to those done for pPDM (above), were done to ensure that eqs 8 and 12–14 are suitable for data analysis. The affinity of S1 and the S1·nucleotide complexes for PM binding noncovalently before it reacts with Cys-707 was estimated from the dependence of the rates of the reaction on [PM]. The apparent rate of increase in activity was measured for an increasing [nucleotide] in each case. The data for S1·MgADP are shown in Figure 3. The midpoint of the increase was used to estimate an apparent dissociation constant for the prereaction complex. In all cases, the apparent  $K_D < 60$   $\mu$ M (Table 2). PM binding to S1 appears to be weaker than that of the larger pPDM, although the  $K_D$  data are not very precise. Plots of the type shown in Figure 4A–C were identical, within experimental error, for a [PM] of 100 and 200  $\mu$ M (data not shown), indicating that Scheme 2 is valid. All the reported data is for a [PM] of 200  $\mu$ M, to make the effective maleimide concentration comparable to 100  $\mu$ M pPDM.

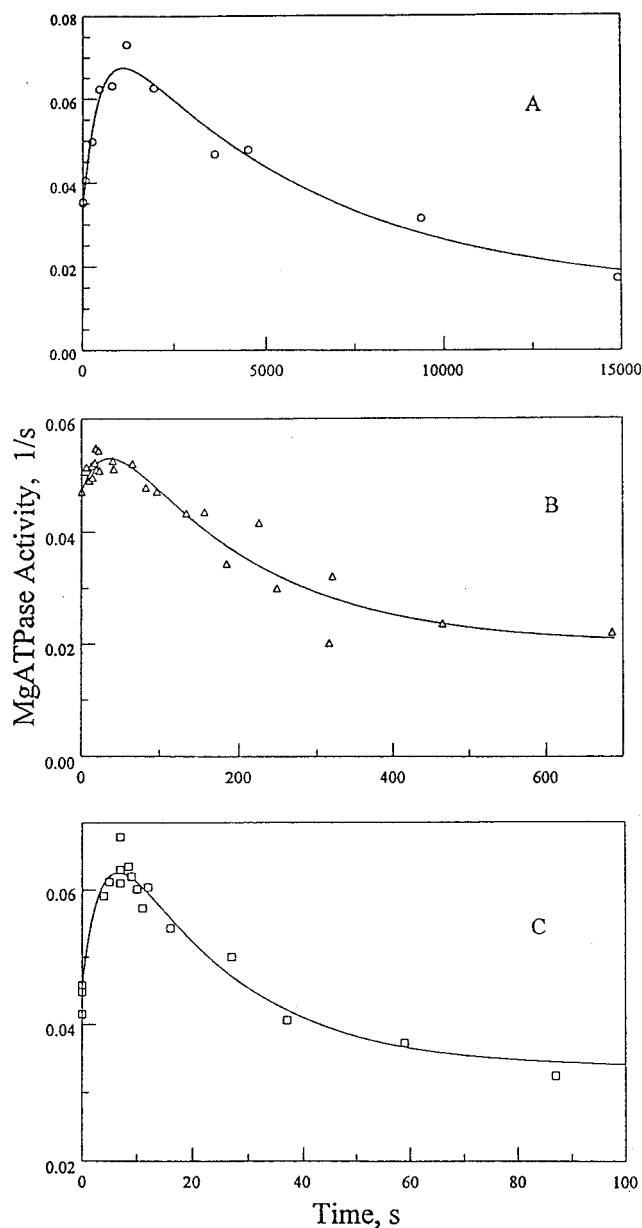


FIGURE 4: PM modification of S1, S1·MgADP, and S1·MgATP. The reaction was started by adding 200  $\mu$ M PM to 10  $\mu$ M S1 at 2  $^{\circ}$ C in 50 mM MOPS, 25 mM Mg(OAc)<sub>2</sub>, 100 mM KOAc, and nucleotide at the concentrations indicated. Aliquots were removed and quenched at the time indicated and assayed for MgATPase activity at 25  $^{\circ}$ C: no ligand (circles), 10 mM ATP (triangles), and 0.10 mM ADP (squares). The rate constants  $k_a$  and  $k_i$  were determined (Table 2) as described in the text.

When S1, S1·MgADP, or S1·MgATP is incubated with PM, there is a transient rise in activity followed by a slower decrease, indicating that with this reagent  $k_a$  and  $k_i$  can be measured (Figure 4A–C). The MgATPase activity of the activated PM–S1, determined from fits to the data, was 0.060–0.079 s<sup>-1</sup> (Table 2), which is in the expected range (35). For S1,  $k_i$  is about  $1/10$  of  $k_a$ , and both increase 10- and 100-fold for S1·MgATP and S1·MgADP, respectively (Table 2). With the monofunctional PM, the slower reaction rate constant for Cys-697 can be measured, whereas with pPDM, the high local effective concentration of the tethered second maleimide group makes  $k_i > k_a$ . Clearly  $k_i$  is ligand sensitive.

For PM modification of S1·MgATP $\gamma$ S and S1·MgPP<sub>i</sub>, the activation phase was not observed (Figure 5A,B). This type

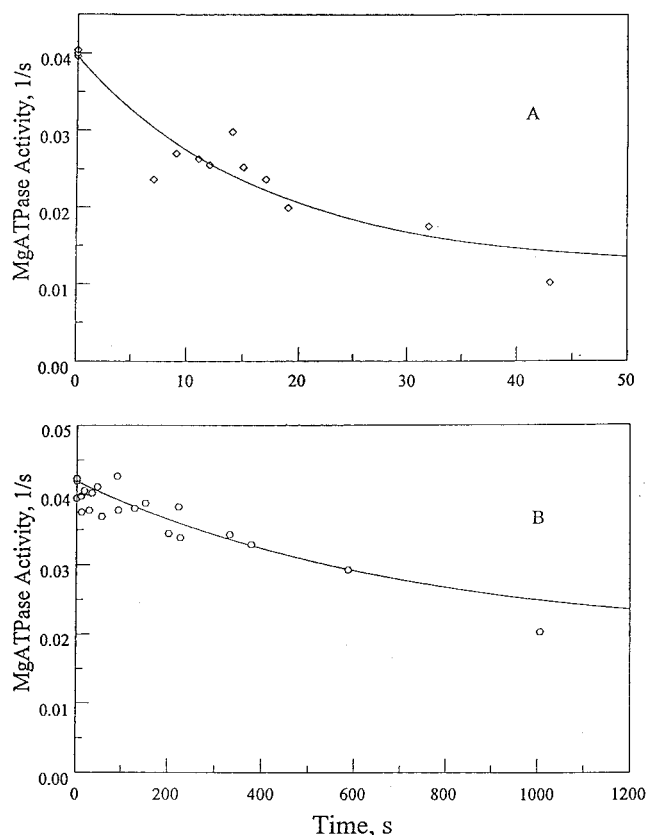


FIGURE 5: PM modification of S1-MgPP<sub>i</sub> and S1-MgATPγS. The reaction was started by adding 200 μM PM to 10 μM S1 at 2 °C in 50 mM MOPS, 25 mM Mg(OAc)<sub>2</sub>, 100 mM KOAc, and nucleotide at the concentrations indicated. Aliquots were removed and quenched at the time indicated and assayed for MgATPase activity at 25 °C: 0.10 mM PP<sub>i</sub> (hexagons) and 0.10 mM ATPγS (diamonds). The rate constants  $k_a$  and  $k_i$  were determined (Table 2) as described in the text.

of time dependence indicates that when these ligands are bound  $k_i > k_a$ , and the rate of inactivation is a measure of  $k_a$  (Table 2), as observed in all cases for pPDM (Figure 1 and Table 1). The rate constant for S1-MgATPγS is larger than that for S1-MgPP<sub>i</sub>, as observed for pPDM. It is notable that this change in the relative values of  $k_a$  and  $k_i$  occurs when the ligand has the  $\beta$  and  $\gamma$  subsites of the ATP site occupied by intact covalently linked phosphoryl (or thiophosphoryl) groups, and presumably also occurs when ATP is bound. The observation that Cys-697 moves to a more exposed hydrophilic environment when ATP binds (Hiratsuka, 1992) is consistent with the changes in  $k_a$  and  $k_i$  observed here when the  $\beta$  and  $\gamma$  subsites are occupied by an intact molecule.

**Tryptophan Intensity Changes.** The qualitatively similar effects of MgATPγS and MgPP<sub>i</sub> on the cysteine reaction rate constants may have other structural manifestations. Tryptophan fluorescence intensity is a method of monitoring S1 structural changes due to nucleotide binding (30). The intensity is sensitive to conditions as well as the ligand bound (31). Steady state tryptophan intensities were measured at 2 °C in the buffer used for cysteine modification for S1 with and without the ligands ADP, ATP, ATPγS, and PP<sub>i</sub> bound, and the percent change was calculated for each case (Table 3). The fluorescence intensity increases observed when S1-MgADP and S1-MgATP form are consistent with earlier reports for S1 at low temperatures which showed that cross-linking does not change the tryptophan fluorescence intensity of S1-MgADP (23). The increase observed when ATPγS

Table 3: Tryptophan Fluorescence Intensity Increases for S1-Nucleotide Complex Formation<sup>a</sup>

ligand	increase (%)
none	(0)
ADP	5.3 ± 1.9
ATP	17.7 ± 1.7
ATPγS	6.3 ± 1.3
PP <sub>i</sub>	1.2 ± 0.1

<sup>a</sup> The steady state fluorescence intensity ( $\lambda_{ex} = 295$  nm,  $\lambda_{em} = 340$  nm) of 1 μM S1 at 3 °C in 50 mM MOPS, 25 mM Mg(OAc)<sub>2</sub>, and 100 mM KOAc was measured before and after addition of each ligand at concentrations that saturate the ATP binding site.

binds is consistent with the increase estimated for ATP before it is hydrolyzed (31). This result is another indication that ATPγS is a suitable analog for ATP in some instances. On the other hand, the intensity increase for PP<sub>i</sub> binding is small and not quantitatively similar to the ATPγS result. Nor do the  $k_a$  values for PM and pPDM modification of S1-MgPP<sub>i</sub> have the same relative values compared to the other nucleotides (Tables 1 and 2). It is not clear which nucleotide PP<sub>i</sub> mimics best. The data suggest that, although the  $\beta$  and  $\gamma$  subsites may control the cross-linking rates, the ATP-induced increase of S1 tryptophan fluorescence intensity requires that the adenine and ribose subsites of the ATP site also be occupied.

## DISCUSSION

**Mechanism of Cross-Linking.** The control measurements made with increasing concentrations of pPDM and PM indicate that prereaction complexes must form, making Schemes 1 and 2 appropriate for analyzing the data. The sulfhydryls of both Cys-697 and Cys-707 are exposed to solution from positions recessed in small crevices on the S1 surface (13), which apparently provide nonspecific binding sites for the reagents. Measurement of the [PM] dependence of the rate of modification of Cys-707 of S1-MgADP, shown in Figure 3, is typical, and in all cases, the pPDM and PM dissociation constants are less than 20 and 60 μM, respectively. The concentrations of pPDM and PM used, 100 and 200 μM, respectively, are high enough to saturate the sites and to ensure that the reagents were negligibly diminished during the reaction, which makes the use of eqs 5–7 and 12–14 appropriate for analyzing the data.

Inactivation by pPDM and PM occurs at rates that are ligand sensitive. The results here are quantitatively consistent with recent data for modifying S1 and S1-nucleotide complexes with fluorescent derivatives (25). The data in Tables 1 and 2 confirm their observation that the reaction rates are as follows: S1-MgADP > S1-MgATP > S1. If the  $k_a$  and  $K_D$  values determined here are used to calculate S1 reaction rates for the concentrations used by Phan et al. (25), the rates are  $5.7 \times 10^{-4} \text{ s}^{-1}$  for PM and  $3.6 \times 10^{-4} \text{ s}^{-1}$  for pPDM, which are reassuringly close to the values of  $7.9 \times 10^{-3}$  and  $3.8 \times 10^{-4} \text{ s}^{-1}$  reported for their reactions at nearly the same pH. A strict comparison of the rates is not possible because the structures of the alkylating reagents are different.

For pPDM,  $k_i > k_a$ , so only  $k_a$  can be determined from the data (Figure 1). A mechanism that is consistent with the data is one in which nucleotide determines the rate constant by changing the relative positions of Cys-707 and the noncovalently bound pPDM in the prereaction complex.

Movement of the helix that includes Cys-707 away from the bulk of the S1 structure when ADP and  $\text{AlF}_4$  are bound to crystalline S1 (14) indicates that nucleotide binding can change the orientation of the Cys-707 sulfhydryl relative to its surroundings. Nucleotide-induced changes in probe mobility (5) and in collisional quenching of Trp-510 fluorescence intensity (24) are consistent with changes in the structure of the crevice around Cys-707. In solution, S1 complexes are structurally dynamic (32, 33), and the reacting conformation for a given pPDM•S1-nucleotide complex may be one of several conformations in equilibrium.

The fact that  $k_i > k_a$  for the pPDM reactions raises the possibility that, once Cys-707 is modified, the native structure is denatured, and  $k_i$ , for cross-linking Cys-697, is the same for all pPDM–S1 species. However, the PM data indicate that the Cys-697/Cys-707 region is not denatured, as  $k_i$  is also ligand sensitive (Table 2). This result is consistent with the report that, when Cys-697 alone is modified, it moves in response to nucleotide (6). The fact that  $k_a > k_i$  for PM reacting with S1, S1•MgADP, and S1•MgATP but  $k_a < k_i$  for S1•MgATP $\gamma$ S and S1•MgPP $_i$  is strong evidence that S1 with Cys-707 modified has an allosteric connection between the ATP site and the Cys-697/Cys-707 region that is still functioning. It is likely that  $k_i$  for pPDM is also ligand-dependent.

This ligand dependence of  $k_i$  could be due to each S1–nucleotide complex existing as a single conformation with the cysteines a specific distance apart, which determines the rate constant. The cross-linking properties and atomic structures do correlate with each other (25). However, single conformations with specific different inter-cysteine distances seem unlikely given the constant distance between Cys-707 and Cys-697 observed in the atomic structures (14–16). A more plausible mechanism is one where each complex consists of a dynamic distribution of reactive and nonreactive conformations, with the distribution being changed depending on which nucleotide is bound. The dynamic nature of the structures of S1 and S1–nucleotide complexes in solution (32, 33) is consistent with each complex existing as exchanging conformations. The fact that cross-linking S1•MgADP is possible with a range of cross-linker lengths (10–12, 34) requires that a complex be able to assume many conformations with differing inter-cysteine distances or, more likely, that one of a few conformations in equilibrium has the cysteines in a flexible loop that allows a variety of distances between them to coexist. In fact, a loop structure was predicted from the primary sequence (38). The fraction of time that S1 spends in this hypothetical loop conformation would be determined by the nucleotide bound. This structural model having S1–nucleotide complexes existing as distributions of conformations, including ones having loop structures in the Cys-697/Cys-707 region, reconciles the ligand-dependent cross-linking rate data here with both the data for variable length cross-linkers (11, 34) and the atomic structures of S1 and S1–nucleotide complexes with unchanged helical Cys-697/Cys-707 regions (14–16).

**Relation to Muscle Function.** Cysteine modification is not part of the actin•S1 ATP hydrolysis cycle, and it is possible that modifying Cys-707 changes S1 structural dynamics. Nonetheless, if the helix to loop structural change proposed above to reconcile the nucleotide dependence of cross-linking kinetics with cross-linker length independence and the  $\alpha$ -helical atomic S1–nucleotide structures is correct, it may

be relevant to muscle function. It is notable not only that the rate constant for pPDM cross-linking to S1•MgATP $\gamma$ S is the largest but also that the rate constants for the intermediates in the ATP hydrolysis cycle that occur before it (actin•S1) and after it (S1•MgADP•P $_i$ ) are the smallest (Table 1). If cross-linking rate constant increases do reflect increases in the time the S1 conformation has a Cys-697/Cys-707 loop, then the data (Table 1) suggest S1•MgATP has the most of this conformation. This proposed correlation between bound unhydrolyzed ATP and a loop in the Cys-697/Cys-707 region suggests a mechanism for using the free energy available from ATP binding to reversibly destabilize S1 in the actin•S1 complex. Specifically, ATP binding to actin•S1 is hypothesized to transform the Cys-697/Cys-707 region from a lower-energy  $\alpha$ -helix surrounded by stabilizing S1 structure to a higher-energy loop that is exposed to the solvent. In solution, naked polypeptide  $\alpha$ -helices and random coils are typically similar in energy, but nucleotide binding to S1 can move the Cys-697/Cys-707 helical region away from its stabilizing tertiary structural environment and toward the solvent (14). This movement of the  $\alpha$ -helix would be expected to make formation of a loop more likely. There are 21 amino acids in two helices that span His-688–Arg-708 (13). If each contributed 0.5 kcal/mol for the hypothesized ATP-induced helix to loop transition, a substantial portion of the ATP binding energy would be stored. At the His-688 end of the helices is a 10-amino acid structure that “caps” the  $\gamma$ -phosphoryl end of the ATP site (13), which provides a plausible physical connection between the ATP site and the helical region. Once S1•MgATP was free of actin, the hypothesized loop conformation would diminish as the  $\alpha$ -helices were reestablished and S1•MgADP•P $_i$  assumed its actin-binding conformation.

## ACKNOWLEDGMENT

We thank Lenard Peller for helpful discussions about and comments on the analysis of the kinetic data.

## REFERENCES

1. Tong, S. W., and Elzinga, M. (1990) *J. Biol. Chem.* 265, 4893–4901.
2. Maita, T., Yajima, E., Nagata, S., Miyaniishi, T., Nakayama, S., and Matsuda, G. (1991) *J. Biochem. (Tokyo)* 110, 75–87.
3. Yamaguchi, J., and Sekine, T. (1966) *J. Biochem.* 59, 24–30.
4. Reisler, E. (1982) *Methods Enzymol.* 85, 84–93.
5. Seidel, J. C., Chopek, M., and Gergely, J. (1970) *Biochemistry* 9, 3265–3272.
6. Hiratsuka, T. (1992) *J. Biol. Chem.* 267, 14941–14948.
7. Hiratsuka, T. (1993) *J. Biol. Chem.* 268, 24742–24750.
8. Botts, J., Takashi, R., Torgerson, P., Hozumi, T., Muhrad, A., Mornet, D., and Morales, M. F. (1984) *Proc. Natl. Acad. Sci. U.S.A.* 81, 2060–2064.
9. Reisler, E., Burke, M., Himmelfarb, S., and Harrington, W. F. (1974) *Biochemistry* 13, 3837–3840.
10. Wells, J. A., and Yount, R. G. (1979) *Proc. Natl. Acad. Sci. U.S.A.* 76, 4966–4970.
11. Burke, M., and Reisler, E. (1977) *Biochemistry* 16, 5559–5563.
12. Wells, J. A., and Yount, R. G. (1980) *Biochemistry* 19, 1711–1717.
13. Rayment, I., Rypniewski, W. R., Schmidt-Base, K., Smith, R., Tomchick, D. R., Benning, M. M., Winkelmann, D. A., Wesenberg, G., and Holden, H. M. (1993) *Science* 261, 50–58.
14. Fisher, A., Smith, C. A., Thoden, J. B., Smith, R., Sutoh, K., Holden, H. M., and Rayment, I. (1995) *Biochemistry* 34, 8960–8972.

15. Smith, C. A., and Rayment, I. (1995) *Biochemistry* 34, 8973–8981.
16. Smith, C. A., and Rayment, I. (1996) *Biochemistry* 35, 5404–5417.
17. Nauss, K. M., Kitagawa, S., and Gergely, J. (1969) *J. Biol. Chem.* 244, 755–765.
18. Margossian, S. S., and Lowey, S. (1982) *Methods Enzymol.* 85, 55–71.
19. Weeds, A. G., and Taylor, R. S. (1975) *Nature* 257, 54–56.
20. Highsmith, S. (1997) *Biochemistry* 36, 2010–2016.
21. Spudich, J. A., and Watt, S. (1971) *J. Biol. Chem.* 246, 4866–4871.
22. Imamura, K., Tada, M., and Tonomura, Y. (1966) *J. Biochem. (Tokyo)* 59, 280–289.
23. Kirshenbaum, K., Papp, S., and Highsmith, S. (1993) *Biophys. J.* 65, 1121–1129.
24. Park, S., Ajtai, K., and Burghardt, T. P. (1997) *Biochemistry* 36, 3368–3372.
25. Phan, B. C., Peyser, Y. M., Reisler, E., and Muhlrads, A. (1997) *Eur. J. Biochem.* 243, 636–642.
26. Bagshaw, C. R., and Trentham, D. R. (1974) *Biochem. J.* 141, 331–349.
27. Sleep, J. A., Trybus, K. M., Johnson, K. A., and Taylor, E. D. (1981) *J. Muscle Res. Cell Motil.* 2, 373–399.
28. Resetar, A. M., and Chalovich, J. M. (1995) *Biochemistry* 34, 16039–16045.
29. Duke, J., Takashi, R., Ue, K., and Morales, M. F. (1976) *Proc. Natl. Acad. Sci. U.S.A.* 73, 302–306.
30. Werber, M. M., Szent-Gyorgyi, A. G., and Fasman, G. D. (1972) *Biochemistry* 11, 2872–2883.
31. Trentham, D. R., Eccleston, J. F., and Bagshaw, C. R. (1976) *Q. Rev. Biophys.* 9, 217–281.
32. Eden, D., and Highsmith, S. (1997) *Biophys. J.* 73, 952–958.
33. Highsmith, S., Akasaka, K., Konrad, K., Goody, R., Holmes, K., Wade-Jardetzky, N., and Jardetzky, O. (1979) *Biochemistry* 18, 4238–4244.
34. Wells, J. A., Knoeber, C., Sheldon, M. C., Werber, M. M., and Yount, R. G. (1980) *J. Biol. Chem.* 255, 11135–11140.
35. Botts, J., Ue, K., Hozumi, T., and Samet, J. (1979) *Biochemistry* 18, 5157–5163.
36. Seidel, J. C. (1973) *Arch. Biochem. Biophys.* 157, 588–596.
37. Xie, L., Li, W. X., Barnett, V. A., and Shoenberg, M. (1997) *Biophys. J.* 72, 858–865.
38. Elzinga, M., and Collins, J. H. (1977) *Proc. Natl. Acad. Sci. U.S.A.* 74, 4281–4284.

BI9713759